The Influence of Local Irregularities on the Vehicle–Track Interaction

Aditi Kumawat, Ullrich Martin, Sebastian Bahamon, and Sebastian Rapp

Abstract Local track irregularities such as mud spots generally cause a sudden variation in track stiffness, which leads to the track geometry degradation in a short period. The interaction of the moving train with such track defects induces additional dynamic stresses in the track system that may prove harmful for the structural health of the track structure. In this paper, an analytical approach is proposed to simulate the vertical track acceleration caused by a local track irregularity when subjected to a uniformly moving load. The railway track is modeled as an infinitely long continuous Euler–Bernoulli beam lying over a Pasternak-type viscoelastic foundation track model. At any given location along the rail beam, the stiffness and thickness of the considered foundation model, respectively, denote the track substructural stiffness and track geometry. To simulate the effects of local irregularities, a pre-defined variation of the stiffness and thickness is considered in a particular section of the foundation model. The time-domain deflection/acceleration responses are obtained for the railway track subjected to a uniformly moving (a) point load and (b) two-mass oscillator system. The results show that the local irregularities may cause significant damage to track structure, which may lead to poor ride comfort or in some cases, even derailment.

Keywords Local track irregularity · Railway track · Analytical model

1 Introduction

The interaction of the moving train with the vertical imperfections (wheel flats and railhead corrugations), rail discontinuities (crossings, switches, turnouts), or local irregularities (mud spots) results in unstable vibrations [1, 2]. These vibrations

A. Kumawat (✉)
Department of Civil Engineering, Indian Institute of Technology Kanpur, Kanpur 208016, India

U. Martin · S. Bahamon · S. Rapp
Institute of Railway and Transportation Engineering, University of Stuttgart, Pfaffenwaldring 7, 70569 Stuttgart, Germany

E. Tutumluer et al. (eds.), *Advances in Transportation Geotechnics IV*,
Lecture Notes in Civil Engineering 165,
https://doi.org/10.1007/978-3-030-77234-5_20

are detrimental for the long-term performance of the track structure, and to ensure passenger safety, continuous track monitoring is essential.

Track stiffness and vertical track geometry are the two crucial parameters that are often implemented for the quality assessment of in-service railway tracks. The track stiffness is defined as the ratio of the train load to the rail deflection. The track geometry data includes the longitudinal profile, alignment, track gauge, cross-level, and twist. Both the track stiffness and geometry may vary along the length of the track at the transition zones, switches, and crossings [3]. However, local irregularities such as mud spots cause a sudden variation in track stiffness and geometry, which leads to track degradation in a short period. The interaction of the moving train with such track defects induces additional dynamic stresses in the track system that may prove harmful for the structural health of the track.

Track recording vehicles are often used for continuous measurement of stiffness and vertical profile along the length of the railway track [4, 5]. Additionally, acceleration sensors mounted on in-service trains are also employed to recognize the track irregularities along the railway tracks. However, continuous monitoring of railway tracks is costly, disrupts the regular operations, and has not been implemented yet for a vast length of railway networks across the world. Therefore, prior knowledge of the typical acceleration signals due to various track defects under the dynamic train loads is essential to detect the track failures as early as possible [6].

Several studies have simulated the acceleration/displacement response of the rail beam under moving train loads using various analytical and numerical methods [7–9]. However, most of these methods analyze the track assuming a constant track stiffness. Only a few theoretical studies are available in the literature which consider the variation of track stiffness along the track length [10]. Moreover, none of those studies take into account track geometry degradation.

The present study is performed in three parts (see Fig. 1). In this first part of this research, an analytical approach is proposed to simulate the vertical track deflection/acceleration caused by a local track irregularity. In the second part, the track acceleration data is collected via (1) an experimental study performed on a 1:87

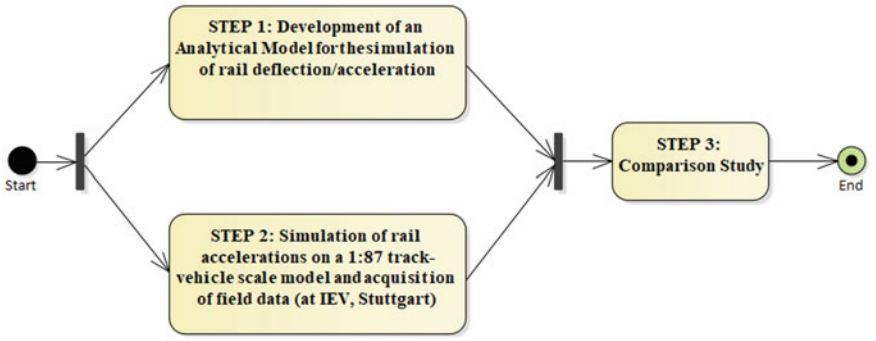

Fig. 1 Activity diagram showing the steps of the study

track–vehicle scale model and (2) field measurements. In the third part, the reliability of the proposed approach will be assessed by comparison with the collected data. In this paper, however, we only present the first part of this study. A subsequent article (under preparation) will focus on the second and third parts based on results of ongoing research.

The railway track is modeled as an infinitely long continuous Euler–Bernoulli beam lying over a Pasternak-type viscoelastic foundation track model. At any given location along the rail beam, the stiffness and thickness of the considered foundation model denote the track substructural stiffness and track geometry, respectively. For simulating the effects of local irregularities, a pre-defined variation of the stiffness and thickness is considered in a particular section of the foundation model. An analytical approach is employed to analyze the response of a vehicle moving over the local irregularity. The results comprise the time-domain deflection/acceleration response of the rail beam and vehicle system for various train velocities.

2 Analysis

Figure 2 represents the railway track model used to analyze the behavior of railway track system under motion-induced dynamic loading. The rail beam is idealized as an infinite Euler–Bernoulli beam with x denoting the space coordinate along the length of the rail beam. The track structure beneath the rail beam is idealized via a viscoelastic Pasternak layer. The viscoelastic component of this layer comprises viscous dampers superimposed with a spring layer. The viscoelastic layer accounts for the stiffness $K(x)$ and damping $c(x)$ associated with various track components (rail pads, sleepers, ballast, and subgrade). Further, the Pasternak layer (of thickness $H_P(x)$) takes into account the shear behavior of the substructure components (ballast

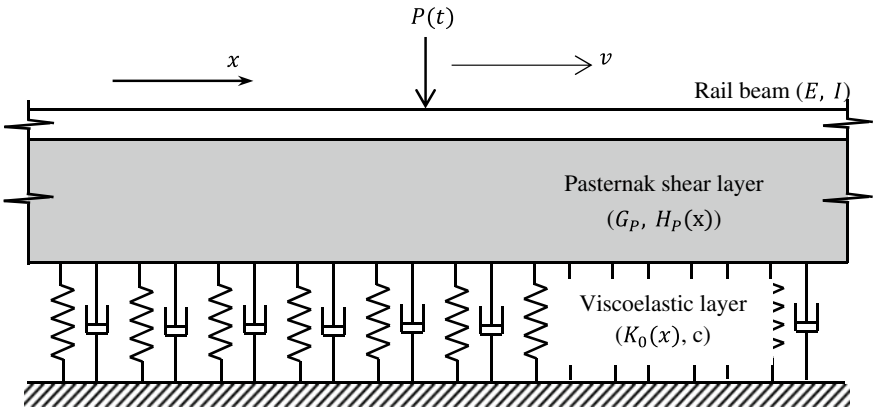

Fig. 2 Definition sketch of the considered railway track model

and subgrade) via the shear parameter $G_P(x)$. In addition to this, the Pasternak shear elements introduce the interaction between the viscoelastic spring elements.

Thus, the considered track model idealizes the railway track system in a simplistic manner through its stiffness, damping, and shear parameters. Ideally, a proper model of the railway track should account for the sleepers, rail pads, and rail fasteners. Further, the model for ballast and subgrade should account for effects such as inter-particle friction, particle angularity, and nonlinear deformation behavior. However, the primary goal of this study is to propose a computationally inexpensive analytical model that, at the cost of certain simplifications, can still yield reasonable results for the reference of practicing engineers.

Under these idealizations, the equation of motion of the rail beam is given by [9]

$$EI\frac{\partial^4 w}{\partial x^4} - G_P(x)H_P(x)\frac{\partial^2 w}{\partial x^2} + K(x)w + c(x)\frac{\partial w}{\partial t} + \rho\frac{\partial^2 w}{\partial t^2} = F(x,t) \quad (1)$$

where $w(x,t)$ is the transverse deflection of the rail beam (considered positive downward), E is Young's modulus of rail beam material, I is the moment of inertia of the rail beam cross section about the axis of bending, ρ is the mass per unit length of the beam, and $F(x,t)$ is the load applied per unit length of the beam. In this case, $F(x,t)$ is given by

$$F(x,t) = P(t)\delta(x - vt) \quad (2)$$

where δ represents Dirac's delta function and $P(t)$ is the time-varying vertical load moving over the rail beam with uniform velocity v. Further, as mentioned in the introduction, the effect of local irregularity (mud spot) is simulated via the variation of stiffness $K(x)$ and height $H_P(x)$ of the Pasternak layer along x. However, it is assumed that the shear parameter $G_P(x)$ and damping values $c(x)$ remain constant along the length of the railway track. Considering that, and using Eq. (2). Equation (1) can be rewritten as:

$$EI\frac{\partial^4 w}{\partial x^4} - G_P H_P(x)\frac{\partial^2 w}{\partial x^2} + K(x)w + c\frac{\partial w}{\partial t} + \rho\frac{\partial^2 w}{\partial t^2} = P(t)\delta(x - vt) \quad (3)$$

Denoting $\iota = \sqrt{-1}$ and $\widehat{f}(\omega)$ as the Fourier transform of an arbitrary function $f(x)$ of the space coordinate x, we have

$$\widehat{f}(\omega) = \int_{-\infty}^{\infty} f(t)\mathrm{e}^{-\iota\omega t}\,\mathrm{d}t \quad (4)$$

and

$$f(t) = \frac{1}{2\pi}\int_{-\infty}^{\infty} \widehat{f}(\omega)\mathrm{e}^{\iota\omega t}\mathrm{d}\omega \tag{5}$$

Further, on taking the Fourier transform of Eq. (3) using Eq. (4) we can write

$$EI\frac{\partial^4\widehat{w}}{\partial x^4} - G_P H_P(x)\frac{\partial^2\widehat{w}}{\partial x^2} + K(x)\widehat{w} + \iota c\omega\widehat{w} - \rho\omega^2\widehat{w} = P\left(\frac{x}{v}\right)\mathrm{e}^{-\iota\omega\left(\frac{x}{v}\right)} \tag{6}$$

where $\widehat{w}(x,\omega)$ denotes the Fourier transform of $w(x,t)$. On simplifying the above equation, we can obtain the solution for $\widehat{w}(x,\omega)$ as:

$$\widehat{w}(x,\omega) = \left(\frac{P(x/v)v^3}{EI\omega^4 + G_P H_P(x)\omega^2 v^2 + v^4 K(x) - \rho\omega^2 v^4 + \iota c\omega v^4}\right)\mathrm{e}^{-i\omega\left(\frac{x}{v}\right)} \tag{7}$$

To obtain the rail beam deflection $w(x,t)$ in time domain, one needs to evaluate the inverse Fourier transform of $\widehat{w}(x,\omega)$ using Eq. (5) as:

$$w(x,t) = \frac{1}{2\pi}\int_{-\infty}^{\infty}\left(\frac{P(x/v)v^3 e^{-i\omega\left(\frac{x}{v}\right)}\mathrm{e}^{\iota\omega t}}{EI\omega^4 + G_P H_P(x)\omega^2 v^2 + v^4 K(x) - \rho\omega^2 v^4 + \iota c\omega v^4}\right)\mathrm{d}\omega \tag{8}$$

Furthermore, to determine the rail beam deflection below the moving load $P(t)$ we can substitute $x = vt$ in the above equation:

$$w_0(t) = \frac{1}{2\pi}\int_{-\infty}^{\infty}\left(\frac{P(t)v^3}{EI\omega^4 + G_P H_P(vt)\omega^2 v^2 + v^4 K(vt) - \rho\omega^2 v^4 + \iota c\omega v^4}\right)\mathrm{d}\omega \tag{9}$$

where $w_0(t)$ represents the rail beam deflection at the location $x = vt$, i.e., $w_0(t) = w(vt,t)$.

3 Results and Discussion

In this section, the response of the railway track system to the local irregularity is evaluated using the above formulation presented. The parameters used for the calculations are listed in Table 1. The variations of the track stiffness from a constant stiffness K_0 (see Table 1) and that of the Pasternak layer thickness H_P (see Table 1) assumed to simulate the local irregularity are shown in Fig. 3a, b, respectively.

Table 1 Railway track and oscillator parameters [2, 8, 9]

Parameters	Symbol	Values
Rail beam		
Mass per unit beam length	ρ	60 kg/m
Modulus of elasticity	E	210 GPa
Central area moment of inertia	I	3055 cm^4
Shear layer		
Shear modulus	G_P	43.3 MPa
Height	H_P	0.5 m
Viscoelastic layer		
Stiffness per unit beam length	K_0	40 MPa
Damping ratio	ζ	0.05
Point load		
Load magnitude	P_0	100 kN
Oscillator		
Mass	m_0	880 kg
	m_1	745 kg
Stiffness	k_1	0.735 MN/m
Coefficient of viscous damping	c_1	9.36 kN-s/m

Figure 4 shows the deflection response $w_0(t)$ of the rail beam subjected to a uniformly moving load $P(t) = P_0$ (see Fig. 2 and Table 1), at the location $x = vt$, where v denotes velocity. It may be noted that the positive value of deflection indicates the downward deflection (i.e., settlement). The deflection is obtained at four different velocities. It may be observed from Fig. 4 that initially, at all the considered velocities, the rail beam deflections are constant. Those constant values are equal to $w_0(t) = w_v$, obtained by inserting the constant stiffness K_0 and thickness H_P in Eq. (9), at the given velocity. However, as the load approaches the local irregularity, the deflection values gradually increase, and respective maximum values are attained at $x = 15$ m. As the load moves beyond the local irregularity, those deflections decrease and again reach the constant value w_v. The increase in deflections (by up to 360%) at the location of local irregularity shows that the stiffness and track geometry degradation may adversely affect the track performance.

Further, it may also be observed from Fig. 4 that as the velocity increases, the maximum deflection at $x = vt$ also increases. To better understand the effect of velocity on the rail beam deflection, Fig. 5 presents the maximum deflections $w_0(t)_{\max}$ observed for the velocities ranging from 0 to 500 m/s. It may be seen that $w_0(t)_{\max}$ increases with velocity, with the maximum amplification occurring at $v = 447$ m/s. This velocity is referred to as the critical velocity of the track. The maximum train velocities for ballasted tracks are much lesser than the observed critical velocity. However, the critical velocity value depends on the overall track stiffness and high

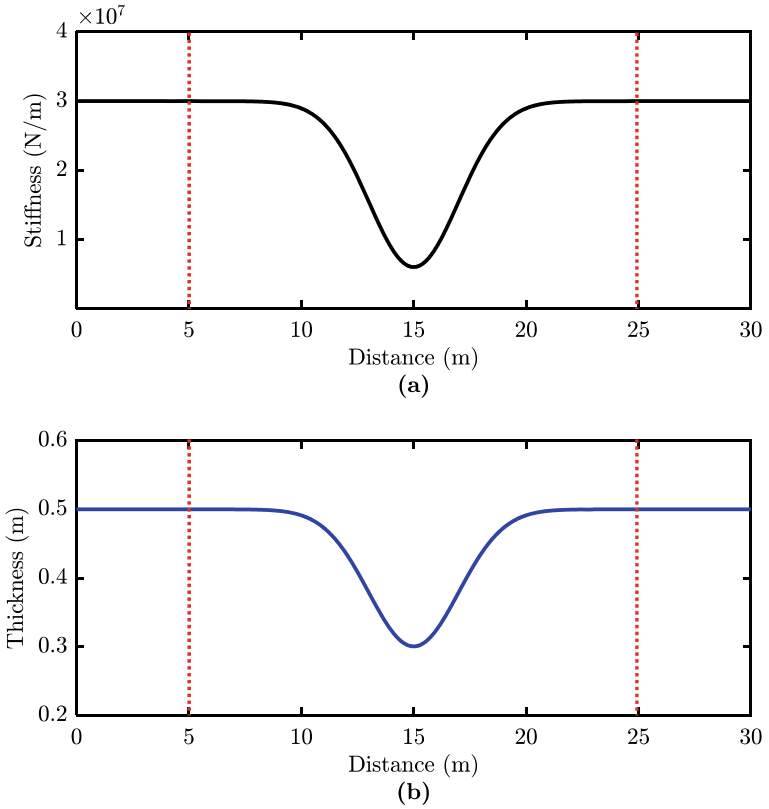

Fig. 3 Variation of track parameters along the railway track. **a** Stiffness. **b** Thickness (the dotted vertical lines specify the location of local irregularity)

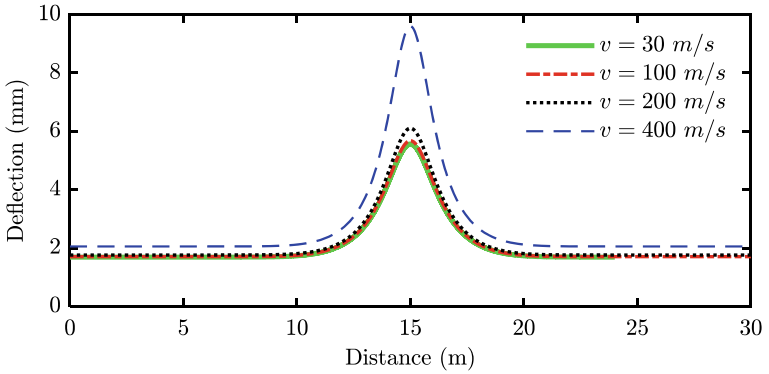

Fig. 4 Deflection response of the rail beam subjected to a uniformly moving load, at the location $x = vt$, for $v = 30$, 100, 200, and 400 m/s

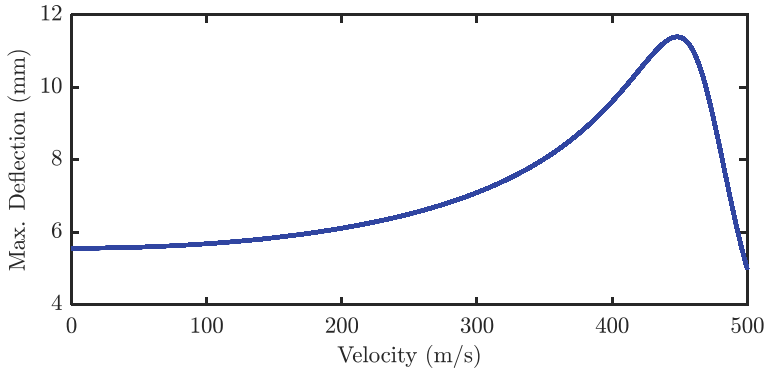

Fig. 5 Maximum rail beam deflections observed for the velocities ranging from 0 to 500 m/s

amplifications in deflections may be observed for a soft subgrade even at velocities of magnitudes comparable with the train velocities [8].

In this section, we analyze the effect of the considered local irregularity on vehicle–track interaction. Figure 6 shows a two-mass oscillator moving uniformly (with velocity v) over the Pasternak viscoelastic model (with varying thickness $H(x)$ and stiffness $K(x)$). The oscillator system comprises masses m_0 and m_1 connected via a spring (with stiffness k_1) and dashpot (with viscous damping coefficient c_1). The parameters defining the oscillator system are listed in Table 1. It is assumed that the moving oscillator system is in constant contact with the rail beam, and therefore, the absolute displacement of mass m_0 is equal to that of the rail beam, i.e., $w_0(t)$. $w_1(t)$ represents the absolute displacement of mass m_1. The force exerted by the moving oscillator system on the rail beam $P(t)$ (see Eq. (9)) is derived in using an approach given in the study [9].

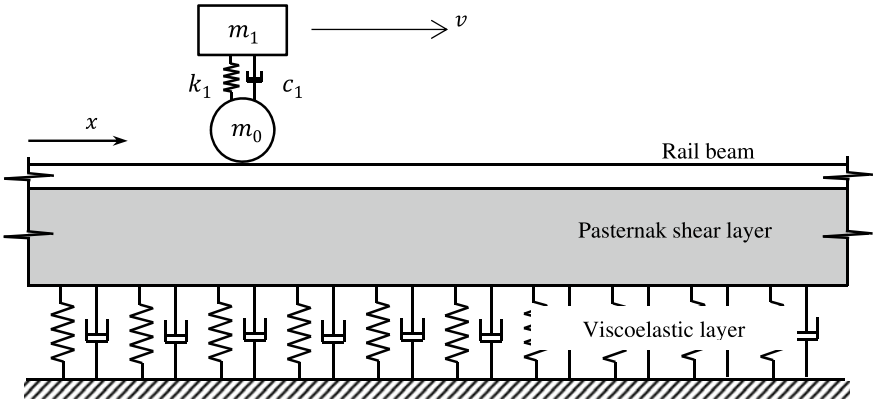

Fig. 6 Railway track model with two-mass oscillator

Figure 7 shows the deflection response of the masses m_0 (or of the rail beam) and m_1 at the location $x = vt$ for three different velocities, $v = 30$, 100, and 200 m/s. It is assumed that both masses are at rest at location $x = 0$ and time $t = 0$.

It may be observed that the deflections $w_0(t)$ and $w_1(t)$ oscillate about a constant value. This value is equal to the deflection observed at the contact point when a point

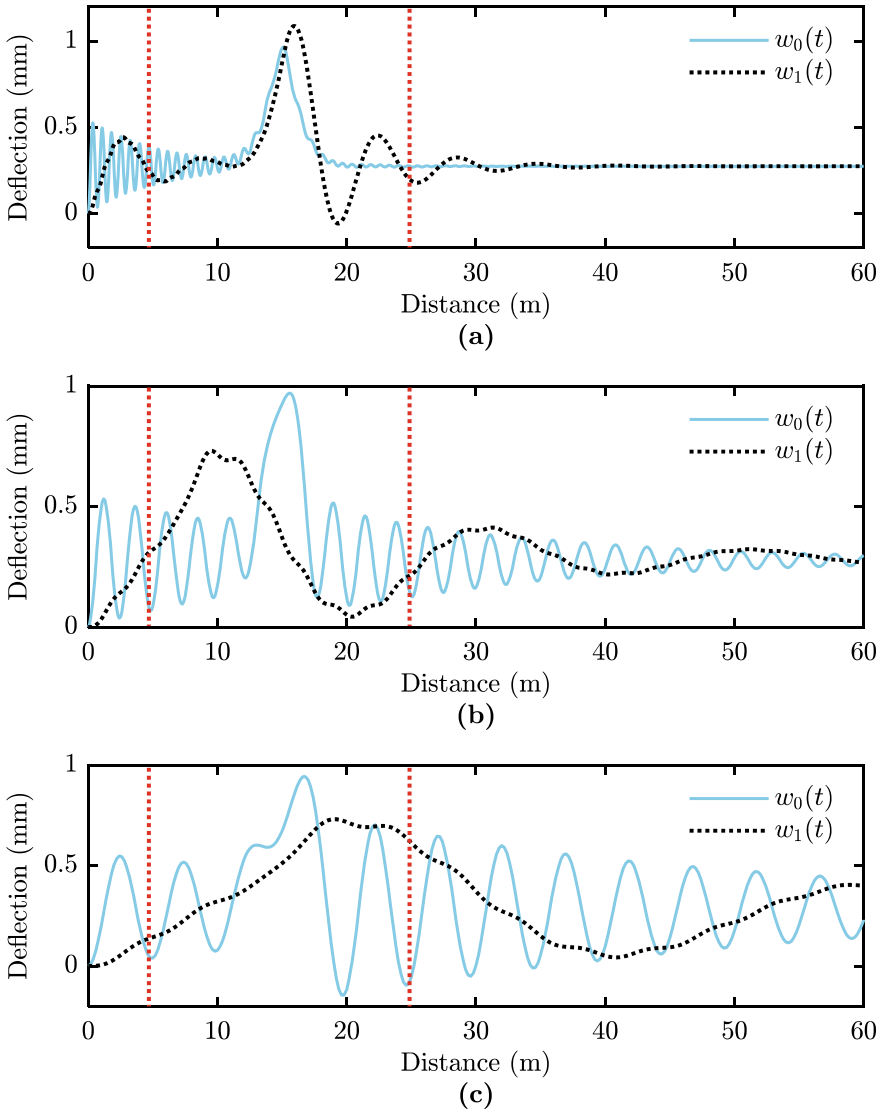

Fig. 7 Deflection responses of the masses m_0 ($w_0(t)$) and m_1 ($w_0(t)$), at $x = vt$, for three different velocities, **a** $v = 30$ m/s, **b** $v = 100$ m/s, and **c** $v = 200$ m/s (the dotted vertical lines specify the location of local irregularity)

load of magnitude $(m_0 + m_1)g$, where g is acceleration due to gravity, traverses the track model. The oscillatory vibrations of the deflection $w_0(t)$ have a much higher frequency than those for the deflection $w_1(t)$. Also, the frequency of vibration for both $w_0(t)$ and $w_1(t)$ decreases with the increase in velocity. Further, the effect of oscillator damping is evident in Fig. 7 where at all the considered velocities, as the oscillator moves away from initial location, the magnitude of deflections $w_0(t)$ and $w_1(t)$ decays with every cycle of vibration. The rate of vibration decay, however, decreases with the increase in velocity.

Further, in Fig. 7, as the oscillator approaches the local irregularity section ($x =$ 5–25 m), an increase (by up to 250%) in $w_0(t)$ can be clearly observed at all velocities. In addition to this, a significant increase (by up to 290%) in $w_1(t)$ may be observed for the velocity $v = 30$ m/s. However, the effect of the local irregularity is negligible on $w_1(t)$ at higher velocities ($v = 100$ and 200 m/s). The low value of deflection observed at higher velocities may be attributed to the local irregularity's length along the rail track. It has been found that for an irregularity of longer length, significant changes in deflections may be observed even at higher velocities. Lastly, as the oscillator moves beyond the local irregularity, the deflection values dampen to the constant value. Thus, it may be concluded that, the local irregularities may cause a significant damage to track structure which may lead to poor ride comfort or, in some cases, derailment.

Figure 8 shows the acceleration responses of the masses m_0 and m_1 along the length of the railway track. The comparison of these responses with the field acceleration data will be able to test the reliability of the presented approach. However, the data acquisition is still in process, and the subsequent article will focus on the comparison study.

4 Summary and Conclusions

In this paper, an attempt was made to simulate the effect of local irregularities in the railway track. The railway track is idealized via a Pasternak viscoelastic foundation model. A pre-defined stiffness and geometry variation are incorporated in a particular section of this foundation model to simulate the local irregularity. Further, an analytical approach is used to analyze the rail beam deflection/acceleration responses under dynamic train loading for the cases of uniformly moving (a) point load and (b) two-mass oscillator system.

For both considered loading types, a significant increase in the rail beam deflections is observed (by up to 360 and 250%, respectively) as the load approaches the simulated local irregularity position. The maximum amplification in the rail beam deflection is observed at the so-called critical velocity value. Lastly, it is found that the oscillator damping brings the rail beam response closer to that observed for the case of constant moving load idealization.

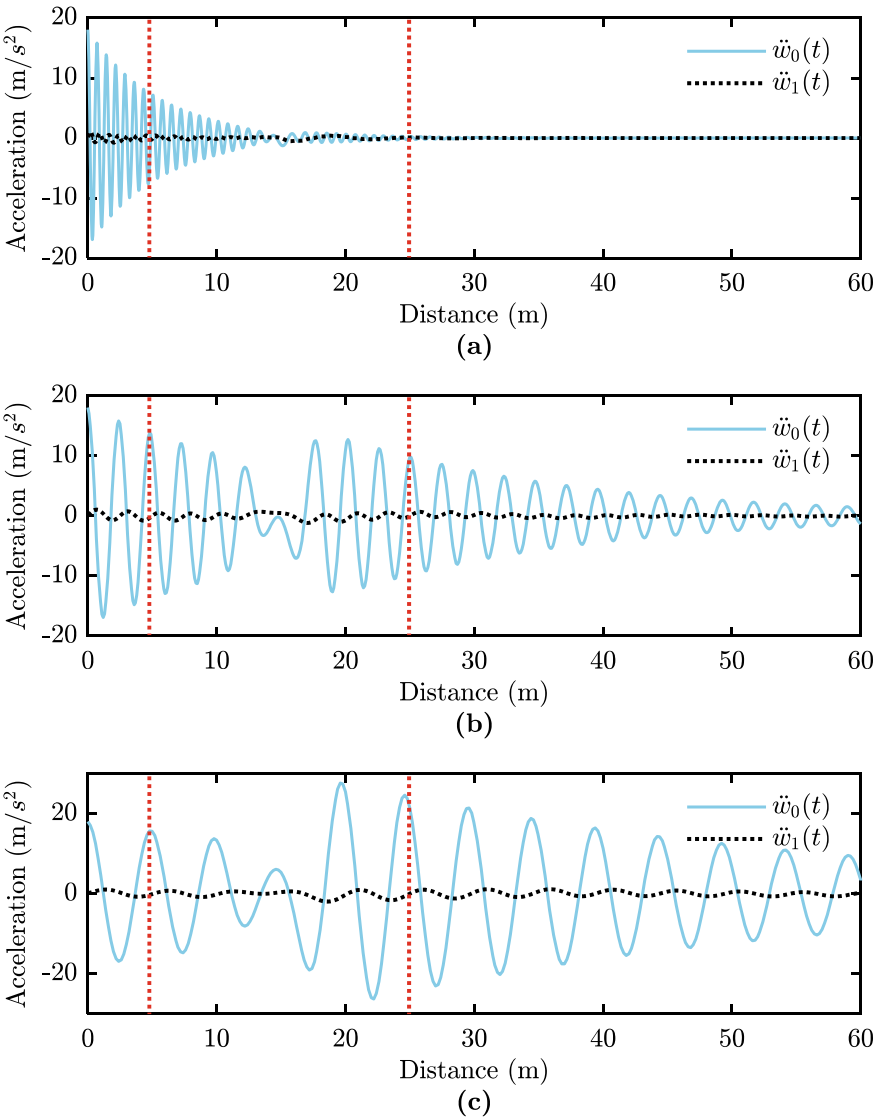

Fig. 8 Acceleration responses of the masses m_0 ($\ddot{w}_0(t)$) and m_1 ($\ddot{w}_1(t)$), at $x = vt$, for three different velocities, **a** $v = 30$ m/s, **b** $v = 100$ m/s, and **c** $v = 200$ m/s (the dotted vertical lines specify the location of local irregularity)

References

1. Knothe KL, Grassie SL (1993) Modelling of railway track and vehicle/track interaction at high frequencies. Veh Syst Dyn 22(3–4):209–262

2. Esveld C (2001) Modern railway track, 2nd edn. Delft University of Technology, MRT-Production
3. Iwnicki S (2006) Handbook of railway vehicle dynamics. CRC Press, Boca Raton
4. Norman C et al (2006) Design of a system to measure track modulus from a moving railcar. US Department of Transportation, Federal Railroad Administration, Office of Research and Development
5. Berggren EG, Kaynia AM, Dehlbom B (2010) Identification of substructure properties of railway tracks by dynamic stiffness measurements and simulations. J Sound Vib 329(19):3999–4016
6. Rapp S et al (2019) Track-vehicle scale model for evaluating local track defects detection methods. Transp Geotech
7. Basu D, Kameswara Rao NSV (2013) Analytical solutions for Euler-Bernoulli beam on visco-elastic foundation subjected to moving load. Int J Numer Anal Meth Geomech 37(8):945–960
8. Kumawat A, Raychowdhury P, Chandra S (2019) Frequency-dependent analytical model for ballasted rail-track systems subjected to moving load. Int J Geomech 19(4):04019016
9. Kumawat A, Raychowdhury P, Chandra S (2019) A wave number-based approach for the evaluation of the Green's function of a one-dimensional railway track model. Eur J Mechan A/Solids 103854
10. Quirke P et al (2017) Drive-by detection of railway track stiffness variation using in-service vehicles. Proc Inst Mechan Eng Part F J Rail Rapid Transit 231(4):498–514